Numerical investigation of scour effects on offshore wind turbine monopile foundations under static and cyclic loading

Oytun Ocal
İzmir Institute of Technology, İzmir, Türkiye, oytunocal@std.iyte.edu.tr

Volkan Isbuga
İzmir Institute of Technology, İzmir, Türkiye, volkanisbuga@iyte.edu.tr

Cihan Taylan Akdag
Technische Universität Berlin, Berlin, Germany, akdag@tu-berlin.de

ABSTRACT: Scour around the monopile foundations of offshore wind turbines (OWTs) has emerged as a critical design and maintenance concern due to its significant influence on structural performance and long-term stability. This study investigates the influence of scour on the behavior of monopile foundations through three-dimensional finite element (FE) analyses conducted in PLAXIS 3D using the UBC3D-PLM constitutive model. The numerical model employed herein was previously validated against laboratory experiments reported in an earlier study by the third author, ensuring its reliability. The analyses encompass both static and cyclic loading conditions, simulating the combined effects of wind and wave-induced cyclic loads typically acting on offshore wind turbines. The reference monopile represents a large diameter "XL monopile" with a diameter of D = 9 m and an embedded length of L = 50 m. Following static loading, cyclic loading was applied up to N = 5 cycles to capture the cyclic degradation response. A parametric study was performed by varying scour width and depth to represent different scour slope geometries, allowing for systematic evaluation of how key scour parameters influence foundation response. The primary objective is to assess the initial degradation of lateral stiffness and displacement behavior as a function of scour geometry, thereby addressing a current research gap concerning monopile foundations under cyclic loading. Results are presented in a form to elucidate the effects of scour on monopile response and to provide practical insights for the design and maintenance of OWT monopile foundations subjected to scour-induced degradation.

1 INTRODUCTION

The global shift toward renewable energy has led to a rapid expansion in the use of offshore wind turbines (OWTs) supported by monopiles being the predominant choice for foundation type. However, seabed scour—the erosion of the seabed around monopiles induced by waves and currents—poses a significant threat to the long-term stability and structural performance of these systems (Lin et al., 2014; Li et al., 2021; Menéndez-Vicente et al., 2025). Scour depths can reach up to 1.5 to 2 times the pile diameter, altering the stress distribution in the surrounding soil and substantially reducing the pile's lateral resistance (Lin and Lin, 2019; Li et al., 2021).

Previous studies indicate that scour depth is a critical parameter that can reduce the lateral capacity by a significant amount. The loss of soil resistance around a monopile will affect the lateral stiffness and moment capacity of the foundation (Lin and Lin, 2019; Li et al., 2021). Moreover, foundations of OWTs are subjected to numerous load cycles throughout their design life due to wind and wave loads. The unloading and reloading lateral stiffness are affected by scour, and cyclic loading can cause stiffness degradation (Galavi et al., 2013; Petelas and Galavi, 2013). However, numerical studies mainly focus on the static load conditions, leaving a critical gap concerning the combined effect of static and cyclic loads, as well as the influence of scour on large-diameter monopile foundations.

This paper aims to address this gap by utilizing a 3D finite element model that employs the UBC3D-PLM soil model, which has been validated against laboratory experiments by Akdag and Rackwitz (2023). In this study, parametric numerical analyses were conducted to simulate both static and cyclic loading with five loading cycles under various scour geometries. The reduction in lateral stiffness was investigated to provide a preliminary result of the analyses on the displacement behavior of monopiles with different scour geometries, thereby providing practical insight for the design and maintenance of OWT monopiles exposed to scour.

2 NUMERICAL MODEL

2.1 Geometry and materials

In this study, the identical three-dimensional symmetric finite element mode, which was developed by Akdag and Rackwitz (2023), was implemented. The FE model represents a large-diameter monopile theoretically designed for an 8–9 MW OWT supported by a monopile with a diameter of $D = 9$ m and a diameter-to-thickness ratio of $D/t = 75$, as illustrated in Fig. 1. In addition to this baseline model, scour is introduced around the pile to varying depths to investigate its influence on monopile behavior. The pile is modeled with a total embedded length of 50 m below the seabed and an additional 65 m above the soil surface, while the water level is defined at 45 m. To minimize boundary effects, the soil domain extends 8.5D in the x-direction and 4.5D in the y-direction, with a depth of 3D beneath the pile base.

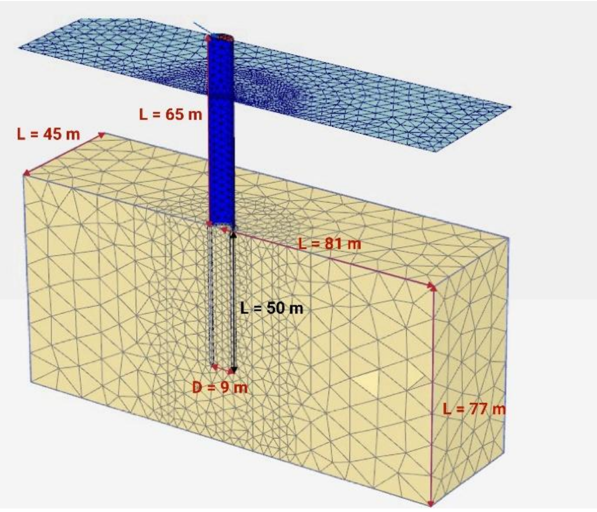

Figure 1. Geometry of the monopile and soil domain without scour.

The material and geometric properties were adopted from Akdag and Rackwitz (2023) and are summarized as follows: a rigid loading plate was modeled at a height of $h = 65$ m with an elastic modulus of $E = 1 \times 10^{16}$ GPa to ensure negligible deformation during the application of lateral and vertical loads. The plate's unit weight and thickness were set to $\gamma = 0.1$ kN/m^3 and $t_{\text{plate}} = 0.05$ m, respectively, to eliminate any mass or stiffness effects. The monopile was modeled as steel with a unit weight of $\gamma = 78$ kN/m^3 and an elastic modulus of $E = 210 \times 10^6$ kN/m^2. Two different soil models were employed depending on the loading conditions. For static loading conditions, the HSsmall model was employed, as it accounts for the nonlinear dependency of stiffness on strain amplitude, even at small strains. The advanced model parameters were adopted based on the recommendations provided in Bentley (2022). Table 1 and Table 2 shows parameters of these soil models.

Table 1 Dense sand parameters considered in the FEM analysis for HSsmall model

Parameter	Value
Buoyant unit weight, γ'[kN/m^3]	10.50
Poisson's ratio, ν	0.20
Power for stress level dependency of stiffness, m	0.50
Internal friction angle, φ′[°]	45.8°
Dilation angle, [°]	15.8°
Cohesion, c′, [kN/m^2]	1.10^{-4}
Initial void ratio, $\boldsymbol{e_{init}}$	0.52
Secant stiffness in the standard drained triaxial test, $\boldsymbol{E_{50}}^{\boldsymbol{ref}}$[kN/m^2]	80.10^3
Tangent stiffness for primary oedometer loading, $\boldsymbol{E_{oed}}^{\boldsymbol{ref}}$ [kN/m^2]	53.10^3
Unloading/reloading stiffness at engineering strains, $\boldsymbol{E_{ur}}^{\boldsymbol{ref}}$ [kN/m^2]	240.10^3
Reference shear modulus at very small strains, $\boldsymbol{G_0}$[kN/m^2]	130.10^3
Shear strain at which, $\boldsymbol{G_s}$=0.722 • $\boldsymbol{G_o}, \boldsymbol{\gamma_{0.7}}$ [kN/m^2]	1.10^{-4}
Failure ratio, $\boldsymbol{R_f}$	0.90
Interface, $\boldsymbol{R_{inter}}$	0.57

Table 2 Dense sand parameters considered in the FEM analysis for UBC3D-PLM model.

Parameter	Value
Saturated unit weight, $\boldsymbol{\gamma_{sat}}$ [kN/m^3]	20.50
Poisson's ratio, ν	0.20
Initial void ratio, $\boldsymbol{e_{init}}$	0.52
Elastic bulk modulus factor, $\boldsymbol{k_B^{*e}}$	1025
Elastic shear modulus factor, $\boldsymbol{k_G^{*e}}$	1465
Plastic shear modulus factor, $\boldsymbol{k_G^{*p}}$	6620
Rate of stress-dependency of elastic bulk modulus $\boldsymbol{m_e}$	0.55
Rate of stress-dependency of elastic bulk modulus $\boldsymbol{n_e}$	0.55
Rate of stress-dependency of elastic bulk modulus $\boldsymbol{n_e}$	0.45
Cohesion, c′, [kN/m^2]	1.10^{-4}
Corrected SPT blow count, $(\boldsymbol{N_1})_{\boldsymbol{60}}$	38.50
Peak friction angle, ′ p [°]	45.8°
Constant volume friction angle, $\boldsymbol{\varphi_{cv}}$ [∘]	37.25°
Densification factor	1.0
Fitting parameter to adjust post-liquefaction behavior, $\boldsymbol{f_{Epost}}$	1.0
Failure ratio, $\boldsymbol{R_f}$	0.9
Interface, $\boldsymbol{R_{inter}}$	0.57

For dynamic phases involving cyclic loading, the UBC3D-PLM soil model was performed under undrained conditions, as recommended by Petalas and Galavi (2013), since it can effectively capture the stiffness degradation behavior of dense, non-cohesive soils under dynamic and cyclic loads. The sand layer was treated as fully saturated and no drainage was permitted during the dynamic steps.

Table 3 Scour geometries considered in the study

Scour No	Scour Depth, D_s (m)	Scour Width, W_s (m)
1	4.5	13.5
2	4.5	9
3	4.5	4.5
4	9	4.5
5	13.5	4.5

2.2 Loads

Four critical design load cases for OWTs monopiles have been defined in the literature (Wichtmann, 2005; LeBlanc et al., 2010; Barari et al., 2017; DNV, 2021). Among these, the loading scenario corresponding to the *serviceability limit state* (SLS) was adopted in this study. For operational conditions, a pile head rotation of 0.5° is the serviceability limit state, SLS, which limits the pile head rotation. To apply maximum cyclic load, initially a series of monotonic load analyses were performed. These series static load analyses conducted using HSsmall soil model. In this step a maximum horizontal load corresponded to nearly 0.5° of rotation was obtained as $H = 29MN$. The lateral load applied in the dynamics analyses was chosen as approximately half of this maximum load in terms of cyclic loading for N=5 cycles.

2.3 Scour Geometry

To investigate the effects of scour, a parametric study was conducted using different scour geometries by deactivating the soil around the pile. According to Li et al. (2021), the scour depth in offshore monopile structures can reach up to 1.3 to 2 times the pile diameter. In this study, five different scour geometries were considered to examine the influence of varying geometric parameters, as presented in Table 3. A representative scour geometry is given in Fig.2 where D_s is the depth and W_s is the top scour width.

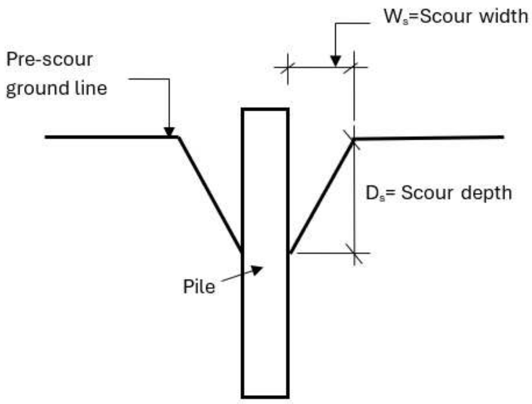

Figure 2. Scour geometry

2.4 Staged Loading Phases

Three-dimensional FE analyses were carried out in several steps. In the initial step, the geostatic stress state was established using the K_0-procedure, which calculates the at-rest earth pressure condition to generate initial stresses in the soil. The next step involved activating the pile and applying the static vertical load. This step was performed as a static analysis with a plastic calculation type, using the HSsmall soil model to accurately capture the stiffness degradation at small deformations. A vertical load of 10 MN was applied at a height of $h = 65$ m, acting at the center of the top rigid plate, consistent with the application carried out by Akdag and Rackwitz (2023). In the subsequent step, scour geometries were introduced by removing soil around the pile to represent different scour conditions, as described in Section 2.3. Cyclic loading was applied as a dynamic step, and the UBC3D-PLM soil model was used for this phase of the analyses. Each loading cycle had a duration of 5 seconds (f=0.2Hz). The maximum deformations were observed at $N = 4.5$ cycles.

3 RESULTS

The results are presented in several forms: (i) normalized displacement at N = 4.5 (22.5 seconds), representing the normalized maximum lateral displacement measured at the midpoint of the pile head; (ii) average pile head rotation over the dynamic loading duration; and (iii) lateral displacement at the midpoint of the pile over the dynamic loading duration.

Figure 3 shows the lateral displacement normalized by the pile diameter, D, normalized lateral displacements, u_x/D, at the midpoint of the pile at N = 4.5. As the scour depth increased while the scour width remained constant, the horizontal displacement values consistently increased. For scour depths of 4.5 m, 9 m, and 13.5 m, the displacement values increased by approximately 2.2, 2.8, and 3.6 times, respectively, for W_s = 4.5 m, compared to the non-scour condition. It was also observed that increasing the scour width while keeping the scour depth constant had no noticeable effect on horizontal displacement, which is an expected outcome since the loss of soil support primarily depends on the depth of material removal rather than the lateral extent of the scour. This result indicates that scour depth is the dominant factor influencing lateral displacement. This finding is consistent with previous studies in the literature (Lin et al., 2014).

Figure 4 illustrates the pile head rotation over five loading cycles (N = 5) for various scour geometries. The results clearly demonstrate that scour depth is the dominant parameter influencing rotational behavior. As the scour depth increases, both the maximum rotation and the overall rotational trend become more pronounced. For scour depths of 4.5 m, 9 m, and 13.5 m, the maximum rotation values increase by approximately 1.15, 1.35, and 1.6 times, respectively, for W_s = 4.5 m compared to the non-scour condition. Similar to the displacement response, the effect of scour on rotation follows the same pattern, with deeper scour conditions leading to greater rotational deformations. The trend also indicates that as the number of loading cycles increases, the cumulative rotation gradually grows and may eventually approach the serviceability limit of 0.5° (DNV, 2021), which is important in the design and maintenance of offshore monopiles.

Figure 5 shows the lateral displacement variation at the pile head over five loading cycles. As the scour depth increases, the maximum lateral displacement under cyclic loading also rises, confirming that scour depth is the dominant parameter. For the most critical scour condition ($D_s = 13.5$ m, $W_s = 4.5$ m), the displacement under loading increased from 0.0710 m at N=0.5 to 0.0809 m at N=4.5, representing an approximate 1.15 times increase over five loading cycles. However, the observed maximum lateral displacement at N=4.5 with the most severe scour assumption used in this study is only $u_{x,\max}/D \approx 0.9\%$. The minimum permanent lateral displacement $u_{x,\min}$ for the deepest scour case changes from $u_{x,\min}/D \approx 0.16\%$ at $N = 1$ to $u_{x,\min}/D \approx 0.26\%$ at $N = 5$. Although cyclic loading amplifies the displacement responses for all cases, such displacements can be considered small compared to the monopile diameter D.

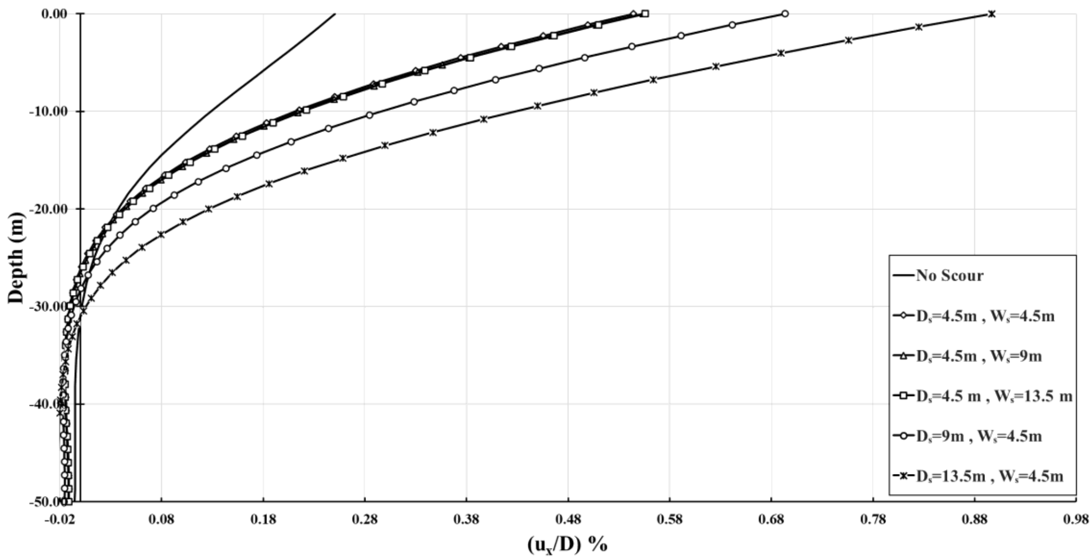

Figure 3. Normalized lateral displacement with various scour geometries.

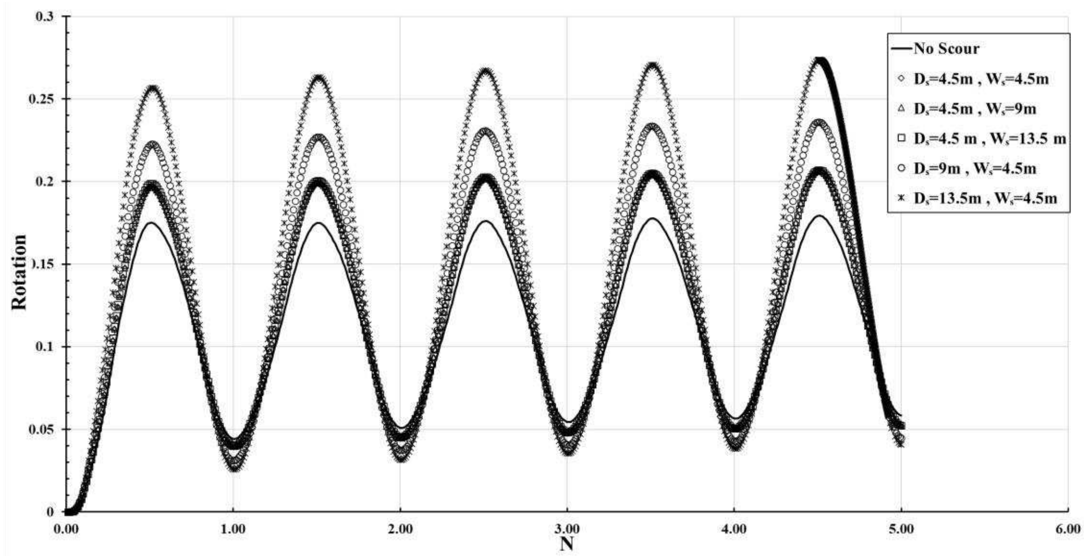

Figure 4. Influence of scour variation on monopile head rotation with number of loading cycles, N.

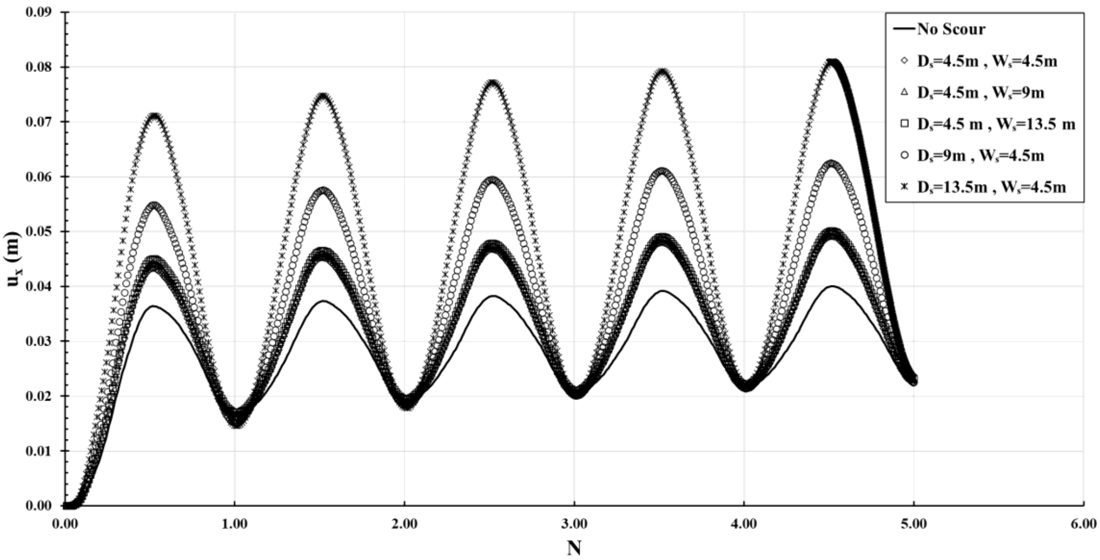

Figure 5. Influence of scour variation on monopile head lateral displacement with number of loading cycles, N

4 CONCLUSIONS

This study investigated the effects of scour on large-diameter monopiles of offshore wind turbines subjected to combined static and cyclic loads. Scour significantly amplifies both rotations and lateral displacements, with scour depth identified as the most influential parameter. Compared to the non-scour condition, lateral displacements increased several-fold, while rotations increased by up to 52% for the deepest scour. Within this range, permanent rotations remained approximately 0.05° after N= 5 cycles for the deepest scour dimension, whereas the maximum rotations went slightly higher than 0.25° still under the 0.5° serviceability limit. Trend analysis indicates that with an increasing number of cycles, these limits could be exceeded, highlighting the need for further investigations considering a higher number of cyclic loadings.

While the results indicate the important influence of scour under combined static and cyclic loading, we note that the cyclic analyses conducted in this study were limited to five cycles, which aim to capture the initial cyclic stiffness degradation and the early-stage response of the monopile–soil system under various scour geometries. Further investigation of long-term cyclic degradation, incorporating higher cycle counts, is needed to provide more representative insights for long-term design.

ACKNOWLEDGEMENTS

The authors are grateful for the financial support provided by funding agency TÜBİTAK. The project presented in this paper is supported by The Scientific and Technological Research Council of Türkiye (TÜBİTAK) under Grant No. 224M248.

REFERENCES

Akdag, C. T., & Rackwitz, F. (2023). Model test and finite element analysis results of a monopile in very dense sand under unidirectional horizontal cyclic loading. *Ocean Engineering*, *288*, 116053.

Barari, A., Bagheri, M., Rouainia, M., and Ibsen, L.B. (2017). Deformation mechanisms for offshore monopile foundations accounting for cyclic mobility effects. *Soil Dynamics and Earthquake Engineering*, 97, 439-453.

Bentley, 2022. Plaxis 3D 2023.1:3-Material Models Manual. https://communities.bentley.com/products/geotechanalysis/w/wiki/46137/manuals—plaxis.

Det Norske Veritas (*DNV). (2021). DNV-ST-0126: Support Structures for Wind Turbines. Det Norske Veritas, Norway*

LeBlanc C, Houlsby G, Byrne B. Response of stiff piles to long-term cyclic lateral load. *Géotechnique* 2010;60(2):7

Q. Li, A. Askarinejad, and K. Gavin. (2021). Impact of scour on lateral resistance of wind turbine monopiles: an experimental study. *Canadian Geotechnical Journal*. **58**(11): 1770-782. https://doi.org/10.1139/cgj-2020-0219

Lin, Y., & Lin, C. (2019). Effects of scour-hole dimensions on lateral behavior of piles in sands. *Computers and Geotechnics*, *111*, 30-41.

Petalas, A., Galavi, V., 2013. Plaxis Liquefaction Model UBC3D-PLM. https://communities.bentley.com/products/geotech-analysis/w/wiki/46116/ubcsand3d-model.

Wichtmann T. *Explicit accumulation model for non-cohesive soils under cyclic loading* Ph.D. thesis, Fakultät für Bauingenieurwesen der Ruhr-Universität Bochum; 2005.

Galavi, V., Petalas, A.L., Brinkgreve, R.B., (2013). Finite element modelling of seismic liquefaction in soils. *Geotech. Eng. J*. SEAGS AGSSEA 44, 55–64.

Menendez-Vicente, C., Lopez-Querol, S., Harris, J. M., & Tavouktsoglou, N. S. (2025). Numerical study on the stiffening properties of scour protection around monopiles for Offshore Wind Turbines. *Engineering Geology*, *345*, 107835.

Lin, C., Han, J., Bennett, C., & Parsons, R. L. (2014). Analysis of laterally loaded piles in sand considering scour hole dimensions. *Journal of Geotechnical and Geoenvironmental Engineering*, *140*(6), 04014024